



# An analytical framework for quantifying aquifer response time scales associated with transient boundary conditions



Farhad Jazaei<sup>a</sup>, Matthew J. Simpson<sup>b,c,\*</sup>, T. Prabhakar Clement<sup>a</sup>

<sup>a</sup>Department of Civil Engineering, Auburn University, Auburn, AL 36849, USA

<sup>b</sup>School of Mathematical Sciences, Queensland University of Technology (QUT), Brisbane, Queensland, Australia

<sup>c</sup>Tissue Repair and Regeneration Program, Institute of Health and Biomedical Innovation, QUT, Brisbane, Queensland, Australia

## ARTICLE INFO

### Article history:

Received 6 June 2014

Received in revised form 3 September 2014

Accepted 8 September 2014

Available online 19 September 2014

This manuscript was handled by Peter K.

Kitanidis, Editor-in-Chief, with the assistance of Adrian Deane Werner, Associate Editor

### Keywords:

Groundwater surface-water interaction

Response time

Steady-state

## SUMMARY

A major challenge in studying coupled groundwater and surface-water interactions arises from the considerable difference in the response time scales of groundwater and surface-water systems affected by external forcings. Although coupled models representing the interaction of groundwater and surface-water systems have been studied for over a century, most have focused on groundwater quantity or quality issues rather than response time. In this study, we present an analytical framework, based on the concept of mean action time (MAT), to estimate the time scale required for groundwater systems to respond to changes in surface-water conditions. MAT can be used to estimate the transient response time scale by analyzing the governing mathematical model. This framework does not require any form of transient solution (either numerical or analytical) to the governing equation, yet it provides a closed form mathematical relationship for the response time as a function of the aquifer geometry, boundary conditions, and flow parameters. Our analysis indicates that aquifer systems have three fundamental time scales: (i) a time scale that depends on the intrinsic properties of the aquifer, (ii) a time scale that depends on the intrinsic properties of the boundary condition, and (iii) a time scale that depends on the properties of the entire system. We discuss two practical scenarios where MAT estimates provide useful insights and we test the MAT predictions using new laboratory-scale experimental data sets.

© 2014 Elsevier B.V. All rights reserved.

## 1. Introduction

Understanding the interactions between groundwater and surface-water systems is an important aspect of water resources management. Using mathematical models to study these interactions can help us better address associated water quality and quantity issues. In the published literature, groundwater and surface-water interactions have been studied using both physical and mathematical approaches (Clement et al., 1994; Winter, 1995; Chang and Clement, 2012; Simpson et al., 2003a) that involve invoking a range modeling simplifications and assumptions, such as assuming that groundwater flow takes place in a homogeneous porous medium, assuming that streams are fully penetrating, and assuming rainfall conditions are uniform. To provide further insight into real-world practical problems, some of these simplifications and assumptions need to be relaxed.

A major challenge in studying groundwater and surface-water interactions arises from the fact that there is a considerable

\* Corresponding author at: School of Mathematical Sciences, Queensland University of Technology (QUT), Brisbane, Queensland, Australia.

E-mail address: [matthew.simpson@qut.edu.au](mailto:matthew.simpson@qut.edu.au) (M.J. Simpson).

difference in the response times of these systems (Rodriguez et al., 2006; Hantush, 2005). For example, after a rainfall event, surface-water levels can respond on the order of hours to days, whereas groundwater levels might respond on the order of weeks to months. Current approaches for studying these problems can be classified into four categories, each of which involve certain limitations: (i) field investigations, which can be expensive and time consuming; (ii) laboratory experiments, which can be limited by scaling issues; (iii) numerical modeling, which, due to the orders of magnitude differences in the response times, might lead to numerical instabilities or other convergence issues (Hantush, 2005); and (iv) analytical modeling, which may be efficient but can have serious limitations in considering practical scenarios involving variations in stream stage, recharge, or discharge boundary conditions (Barlow and Moench, 1998). Several previous researchers have presented analytical solutions focussing on aquifer response times (Rowe, 1960; Pinder et al., 1969; Singh and Sagar, 1977; Lockington, 1997; Mishra and Jain, 1999; Ojha, 2000; Swamee and Singh, 2003; Srivastava, 2003).

Understanding groundwater response times near a groundwater surface-water boundary will help us make informed decisions about the use of different types of mathematical models. For

example, if the water stage in the surface-water body is perturbed, we expect the local groundwater system in contact with the stream to undergo a transient response and eventually reach a new steady-state. Tools that can predict the time needed for such transient responses to relax to a steady-state condition could help to make informed decisions about using appropriate mathematical models. For example, immediately after changing the surface-water elevation, we would need to apply a transient mathematical model to predict the groundwater response; whereas, after a sufficiently long period of time, we could describe the system using a simpler steady-state model (Simpson et al., 2003b).

In the groundwater literature, *response time* (or lag time) is defined as the time scale required for a groundwater system to change from some initial condition to a new steady-state (Sophocleous, 2012). In the heat and mass transfer literature this time scale is known as the *critical time* (Hickson et al., 2009a,b, 2011). Simpson et al. (2013) summarized several previous attempts to estimate the groundwater response time into three categories: (i) numerical computation, (ii) laboratory-scale experimentation, and (iii) simple mathematical definitions or approximations. All three categories involve making subjective definitions of the response time by tracking transient responses and choosing an arbitrary tolerance  $\epsilon$  and claiming that the response time is the time taken for the transient response to decay below this tolerance (Chang et al., 2011; Landman and McGuinness, 2000; Watson et al., 2010; Hickson et al., 2011; Lu and Werner, 2013). There are several limitations with this approach. The most obvious limitation is that the response time depends on a subjectively defined tolerance,  $\epsilon$ . Secondly, this approach does not lead to a general mathematical expression to describe how the response time would vary with problem geometry, changes in boundary conditions or aquifer parameters. Finally, this approach requires an analytical or a numerical solution to the governing transient equation. To deal with these limitations, Simpson et al. (2013) demonstrated the use of a novel concept, mean action time (MAT), for estimating aquifer response times.

The concept of MAT was originally proposed by McNabb and Wake (1991) to describe the response times of heat transfer processes. MAT provides an objective definition for quantifying response time scales of different processes (McNabb, 1993). MAT analysis leads to an expression relating the response time to the various model parameters. Simpson et al. (2013) used MAT to characterize the response time for a groundwater flow problem that was driven by areal recharge processes, but did not consider any groundwater and surface-water interactions. The objective of this study is to extend the work of Simpson et al. (2013) and present a mathematical model which describes transient groundwater flow processes near a groundwater and surface-water boundary with time-dependent boundary conditions. We adapt existing MAT theory to deal with time-dependent boundary conditions and present expressions for MAT which describe spatial variations in response times for both linear and non-linear boundary forcing conditions. These theoretical developments are then tested using data sets obtained from laboratory experiments.

## 2. Mathematical development

We consider a one-dimensional, unconfined, Dupuit–Forchheimer model of saturated groundwater flow through a homogeneous porous medium (Bear, 1979), which can be written as,

$$S_y \frac{\partial h}{\partial t} = K \frac{\partial}{\partial x} \left[ h \frac{\partial h}{\partial x} \right], \quad (1)$$

where  $h(x, t)$  (L) is the groundwater head at position  $x$ ,  $t$  (T) is time,  $S_y$  (-) is the specific yield and  $K$  (L/T) is the saturated hydraulic

conductivity. When variations in the saturated thickness are small compared to the average saturated thickness, we can linearize the governing equation by introducing an average saturated thickness,  $\bar{h}$ , to yield (Bear, 1979),

$$S_y \frac{\partial h}{\partial t} = K \bar{h} \frac{\partial^2 h}{\partial x^2}, \quad (2)$$

which can be re-written as the linear diffusion equation,

$$\frac{\partial h}{\partial t} = D \frac{\partial^2 h}{\partial x^2}, \quad (3)$$

where  $D = K\bar{h}/S_y$  ( $L^2/T$ ) is the aquifer diffusivity. In this work, we will use Eq. (3) to model a groundwater system which changes from an initial condition,  $h(x, 0) = h_0(x)$ , to some steady-state,  $\lim_{t \rightarrow \infty} h(x, t) = h_\infty(x)$ . We will consider two different classes of boundary conditions for Eq. (3): Case 1, in which both the left ( $x = 0$ ) and right ( $x = L$ ) boundary conditions vary as functions of time, and Case 2, in which one boundary condition is fixed and the other one is allowed to vary with time.

### 2.1. Case 1: two time varying boundary conditions

We first consider the case where the surface-water variations at both the left ( $x = 0$ ) and right ( $x = L$ ) boundaries vary with time,

$$B_L(t) = h(0, t), \quad (4)$$

$$B_R(t) = h(L, t). \quad (5)$$

We assume that, after a sufficient amount of time, both  $B_L(t)$  and  $B_R(t)$  approach some steady condition,

$$\lim_{t \rightarrow \infty} B_L(t) = h_\infty(0), \quad (6)$$

$$\lim_{t \rightarrow \infty} B_R(t) = h_\infty(L), \quad (7)$$

for which the steady solution of Eq. (3) is,

$$h_\infty(x) = \left( \frac{h_\infty(L) - h_\infty(0)}{L} \right) x + h_\infty(0). \quad (8)$$

A schematic of these initial, transient and steady-state conditions are shown in Fig. 1.

The purpose of this study is to present an objective framework to estimate the time scale required for the system to effectively relax to steady-state conditions. To begin our analysis we first consider the following two mathematical quantities (Ellery et al., 2012a,b; Simpson et al., 2013),

$$F(t; x) = 1 - \frac{[h(x, t) - h_\infty(x)]}{[h_0(x) - h_\infty(x)]}, \quad t \geq 0, \quad (9)$$

$$f(t; x) = \frac{dF(t; x)}{dt} = - \frac{\partial}{\partial t} \left[ \frac{h(x, t) - h_\infty(x)}{h_0(x) - h_\infty(x)} \right], \quad t \geq 0, \quad (10)$$

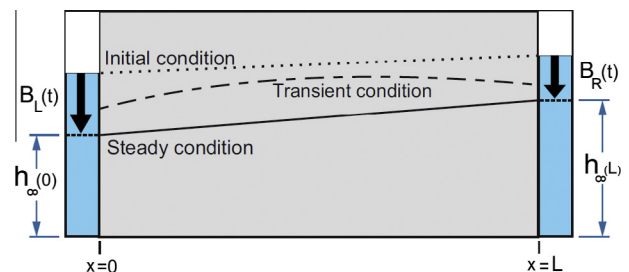


**Fig. 1.** Schematic of the physical model showing initial (dotted), transient (dashed) and steady (solid) conditions. Changes in water head in the right and left boundaries are defined by functions of  $B_R(t)$  and  $B_L(t)$ , respectively. At steady-state, the left and right boundary conditions reach the levels  $h_\infty(0)$  and  $h_\infty(L)$ , respectively.

where  $h(x, t)$  is the solution of Eq. (3),  $h_0(x)$  is the initial groundwater level, and  $h_\infty(x)$  is the steady-state level reached after a sufficiently long period of time and we require that  $h_0(x) \neq h_\infty(x)$ , ensuring that a transition takes place. Theoretically, the transient response will require infinite amount of time to reach steady-state. This implies that at all spatial locations,  $F(t; x)$  changes from  $F = 0$  at  $t = 0$  to  $F \rightarrow 1^-$  as  $t \rightarrow \infty$ . We can interpret  $F(t; x)$  as a cumulative distribution function (CDF) and  $f(t; x)$  as a probability density function (PDF) (Ellery et al., 2012a,b; Simpson et al., 2013).

The MAT,  $T(x)$ , is the mean or the first moment of  $f(t; x)$ , which can be written as (Simpson et al., 2013),

$$T(x) = \int_0^\infty tf(t; x) dt. \tag{11}$$

To solve for  $T(x)$ , we apply integration by parts to Eq. (11) and make use of the fact that  $h(x, t) - h_\infty(x)$  decays to zero exponentially fast as  $t \rightarrow \infty$  (Haberman, 2004; Ellery et al., 2012a,b) to give,

$$T(x)g(x) = \int_0^\infty h_\infty(x) - h(x, t) dt, \tag{12}$$

where we define  $g(x) = h_\infty(x) - h_0(x)$ . Differentiating Eq. (12) twice with respect to  $x$  and combining the result with Eq. (3) yields,

$$\frac{d^2[T(x)g(x)]}{dx^2} = -\frac{g(x)}{D}. \tag{13}$$

Expanding Eq. (13) by applying the product rule gives,

$$\frac{d^2T(x)}{dx^2} + \frac{dT(x)}{dx} \left[ \frac{2}{g(x)} \frac{dg(x)}{dx} \right] + T(x) \left[ \frac{1}{g(x)} \frac{d^2g(x)}{dx^2} \right] = -\frac{1}{D}. \tag{14}$$

which is a differential equation that governs the MAT for any change from  $h_0(x)$  to  $h_\infty(x)$ , provided that  $F(t; x)$  monotonically increases from  $F = 0$  at  $t = 0$  to  $F = 1^-$  as  $t \rightarrow \infty$ .

To solve Eq. (14), we must specify boundary conditions at  $x = 0$  and  $x = L$ . The appropriate boundary conditions can be found by evaluating Eq. (11) at  $x = 0$  and  $x = L$ , recalling that the time variation in head at these locations is given by  $B_L(t)$  and  $B_R(t)$ , respectively. We apply integration by parts, assuming that  $B_L(t)$  and  $B_R(t)$  approach  $h_\infty(0)$  and  $h_\infty(L)$ , respectively, faster than  $t^{-1}$  decays to zero as  $t \rightarrow \infty$ , to give,

$$A = \frac{1}{\alpha} \int_0^\infty (h_\infty(0) - B_L(t)) dt, \quad \text{where } \alpha = h_\infty(0) - h_0(0), \tag{15}$$

$$B = \frac{1}{\beta} \int_0^\infty (h_\infty(L) - B_R(t)) dt, \quad \text{where } \beta = h_\infty(L) - h_0(L). \tag{16}$$

The constants  $A$  and  $B$  represent the mean time scales of the boundary conditions. With these two constants we may solve Eq. (14) to give an expression for the effective time scale of the system,

$$T(x) = \underbrace{\frac{x(L-x)}{6D}}_{\text{Intrinsic time scale of the aquifer}} + \underbrace{\frac{A\alpha(L-x) + B\beta x}{\alpha(L-x) + \beta x}}_{\text{Intrinsic time scale of the boundary conditions}} + \underbrace{\frac{xL(L-x)(\alpha + \beta)}{6D[\alpha(L-x) + \beta x]}}_{\text{Mixed time scale of the system}}. \tag{17}$$

The first term on the right of Eq. (17) is independent of the details of the boundary conditions, and so we interpret it as an *intrinsic time scale of the aquifer*. The second term on the right of Eq. (17) is independent of  $D$ , and depends on the details of the boundary conditions. Therefore, we interpret this term as an *intrinsic time scale of the boundary conditions*. We note that the intrinsic time scale of the boundary conditions can also be interpreted as the weighted average of  $A$  and  $B$ ,  $(Aw_a + Bw_b)/(w_a + w_b)$ , with linear weight functions  $w_a = \alpha(L-x)/L$  and  $w_b = \beta x/L$ . This interpretation implies the influence of the boundary conditions on the

time scale of the process at any point within the system depends on the distances from the boundaries and also on the magnitude of the changes imposed at the boundaries. For example, the time scale at a point close to the left hand boundary,  $x = 0$ , will be dominated by the influence of the time scale of  $B_L(t)$  and relatively unaffected by the influence of the time scale of  $B_R(t)$ , which is as we might expect intuitively. However, intuition alone cannot provide quantitative insight into the impact of the boundary conditions time scales at intermediate locations where the impact of both boundary conditions plays a role. Finally, the third term on the right of Eq. (17) depends on properties of the entire system including both  $D$ , the magnitudes of head changes at the boundaries, but is independent of  $A$  and  $B$ , which are the mean time scales of the boundary conditions. Therefore we consider this third term as the *mixed time scale of the system*.

To provide additional information about the response time we also consider the second moment of  $f(t; x)$ , known as the variance of action time (VAT),  $V(x)$ , and quantifies the spread about the MAT (Ellery et al., 2012b, 2013). VAT is defined as,

$$V(x) = \int_0^\infty (t - T(x))^2 f(t; x) dt. \tag{18}$$

Using integration by parts and noting that  $h(x, t) - h_\infty(x)$  decays to zero exponentially fast as  $t \rightarrow \infty$ , Eq. (18) can be written as,

$$\psi(x) = 2 \int_0^\infty t(h_\infty(x) - h(x, t)) dt, \tag{19}$$

where we have defined  $\psi(x) = g(x)[V(x) + T(x)^2]$ . Differentiating Eq. (19) twice with respect to  $x$  and combining the result with Eq. (3) gives,

$$\frac{d^2\psi(x)}{dx^2} = \frac{-2T(x)g(x)}{D}. \tag{20}$$

To solve Eq. (20), we require two boundary conditions, which are given by,

$$\psi(0) = \alpha(C + A^2), \tag{21}$$

$$\psi(L) = \beta(E + B^2), \tag{22}$$

where  $C$  and  $E$  are the VAT at  $x = 0$  and  $x = L$ , respectively. These constants are defined using Eq. (18), and can be written as,

$$C = \frac{1}{\alpha} \int_0^\infty \frac{dB_L(t)}{dt} (t - A)^2 dt, \tag{23}$$

$$E = \frac{1}{\beta} \int_0^\infty \frac{dB_R(t)}{dt} (t - B)^2 dt. \tag{24}$$

We solve Eq. (20) for  $\psi(x)$ , recalling that  $V(x) = \psi(x)/g(x) - T(x)^2$  and that  $h(x, t) - h_\infty(x)$  decays to zero exponentially fast as  $t \rightarrow \infty$ , which gives us,

$$V(x) = \frac{1}{180D^2(\alpha(L-x) + \beta x)} (\gamma + \delta + \eta) - \theta, \tag{25}$$

where,

$$\begin{aligned} \gamma &= 3x^5(\beta - \alpha) + 15x^4\alpha L + 180\alpha LD^2(C + A^2), \\ \delta &= 10x^3(-\beta L^2 - 6\beta BD + 6DA\alpha - 2\alpha L^2) - 180x^2\alpha LAD, \\ \eta &= x(180D^2(\beta E - \alpha C + \beta B^2 - \alpha A^2) + 60L^2D(\beta B + 2A\alpha) + L^4(7\beta + 8\alpha)), \\ \theta &= \left( \frac{x^3(\beta - \alpha) + 3x^2\alpha L - x(\beta L^2 + 6\beta BD - 6DA\alpha + 2\alpha L^2) - 6\alpha LAD}{6D(x\beta - \alpha x + \alpha L)} \right)^2. \end{aligned} \tag{26}$$

VAT is a measure of the spread of the PDF about the mean (Ellery et al., 2013). A small VAT implies that the spread about the mean is small, and that the MAT is a sufficient estimate of the time required for the system to effectively reach steady-state (Simpson

et al., 2013; Ellery et al., 2013). Alternatively, a large VAT indicates that the PDF has a large spread about the mean and a better estimate of the response time is  $T(x) + \sqrt{V(x)}$  (Simpson et al., 2013; Ellery et al., 2013). This framework gives an explicit estimate for the response time scale required for a groundwater system to respond to a relatively general set of boundary conditions. The method objectively describes the dependence of the time scale on various aquifer parameters ( $K$ ,  $S_y$ ,  $\bar{h}$ ,  $B_L(t)$ ,  $B_R(t)$  and  $L$ ) and does not require any numerical or analytical transient solution of the governing equation.

Our MAT framework involves certain limitations which should be made explicit. The first limitation is that the boundary conditions must vary monotonically with time otherwise our definition of  $F(t; x)$  cannot be interpreted as a CDF. The second limitation is that  $B_L(t)$  and  $B_R(t)$  must asymptote to the corresponding steady values faster than  $t^{-1}$  decays to zero as  $t \rightarrow \infty$ . We also require that  $B_L(t)$  and  $B_R(t)$  both increase or decrease, or that one of the boundary conditions must remain fixed with time. If one boundary condition decreases and the other increases, there will be some points in the domain at which the head distribution does not vary monotonically and  $F(t; x)$  cannot be interpreted as a CDF.

### 2.2. Case 2: one fixed boundary condition and one time varying boundary condition

Here we consider a fixed boundary condition at  $x = 0$  and a time-varying boundary condition at  $x = L$ . We consider the water level variation at  $x = L$  to be given by  $B_R(t) = h(L, t)$ , which eventually asymptotes to some steady value,  $h_\infty(L)$ . As in Case 1, the differential equation governing the MAT is Eq. (14), which, in this case, simplifies to,

$$\frac{d^2 T(x)}{dx^2} + \frac{2}{x} \frac{dT(x)}{dx} = -\frac{1}{D}. \quad (27)$$

Two boundary conditions are required to solve Eq. (27). The boundary condition at  $x = L$  is the same as in Case 1, and given by Eq. (16). To determine the boundary condition at  $x = 0$ , we multiply both sides of Eq. (27) by  $x$ , which gives,

$$x \frac{d^2 T(x)}{dx^2} + 2 \frac{dT(x)}{dx} = -\frac{x}{D}. \quad (28)$$

Evaluating Eq. (28) at  $x = 0$  gives a Neumann boundary condition,  $dT/dx = 0$  at  $x = 0$ . With these boundary conditions the solution of Eq. (27) is,

$$T(x) = \frac{L^2 - x^2}{6D} + B. \quad (29)$$

To find the VAT we have  $\psi(0) = 0$  and  $\psi(L) = \beta(B^2 + E)$  as boundary conditions for Eq. (20). Recalling that  $V(x) = \psi(x)/g(x) - T(x)^2$ , the VAT is given by,

$$V(x) = \frac{L^4 - x^4}{90D^2} + E, \quad (30)$$

where  $\beta$ ,  $B$  and  $E$  are defined by Eqs. (16) and (24), respectively.

### 3. Laboratory experiments

We now examine the validity of the theoretical developments presented in Section 2. To do this we consider two laboratory experiments performed in a rectangular soil tank, using methods described previously (Abarca and Clement, 2009; Simpson et al., 2013; Chang and Clement, 2012). An image of the physical tank is shown in Fig. 2. The tank has three distinct chambers. The central porous media chamber (50 cm × 28 cm × 2.2 cm) was packed under wet conditions with a uniform fine sand. The hydraulic

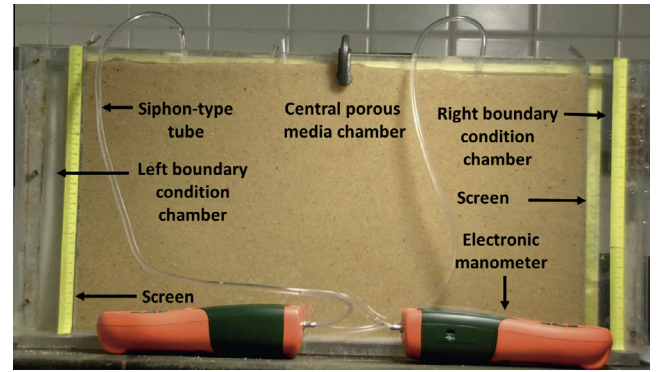


Fig. 2. Experimental aquifer set up used in this study.

conductivity and specific yield of the porous medium are estimated to be 330 m/day and 0.2, respectively. Two chambers at either sides were separated using fine metal screens; these chambers were used to set up the boundary conditions. Our coordinate system is such that  $x = 0$  and  $x = L$  denotes the left and right boundaries, respectively. Siphon-type tubes connected to electronic manometers, shown in Fig. 2, were used to monitor head at two internal points.

#### 3.1. Experiment 1: Laboratory data for Case I

In this experiment, we consider a linearly varying boundary condition at  $x = 0$  and a quadratically varying boundary condition at  $x = L$ . We model the right boundary condition as,

$$B_R(t) = \begin{cases} (h_\infty(L) - h_0(L)) \frac{t}{N} + h_0(L), & 0 \leq t \leq N, \\ h_\infty(L), & t > N, \end{cases} \quad (31)$$

which is a linear change from  $h_0(L)$  to  $h_\infty(L)$  in  $N$  units of time. We model the left boundary condition as,

$$B_L(t) = \begin{cases} at^2 + bt + c, & 0 \leq t \leq M, \\ h_\infty(0), & t > M. \end{cases} \quad (32)$$

which is a nonlinear change from  $h_0(0)$  to  $h_\infty(0)$  in  $M$  units of time.

To represent a linear head variation,  $B_R(t)$ , a pump was used to evacuate water from the right chamber at a uniform rate. To represent a quadratically varying head condition,  $B_L(t)$ , we allow water to drain through an orifice in the left chamber. Using the Bernoulli equation, we derive a quadratic relationship between falling head and drainage time (Bansal, 2005). To specify  $B_L(t)$ , experimental data for water elevation changes occurring at the left boundary were recorded. A quadratic expression,  $B_L(t) = at^2 + bt + c$ , was fitted to the data set. The initial state for the system was set to  $h_0(x) = 22.5$  cm. The left boundary condition set to vary quadratically from  $h_0(0) = 22.5$  cm to  $h_\infty(0) = 19.1$  cm in 3 s, and the right boundary condition to vary linearly from  $h_0(L) = 22.5$  cm to  $h_\infty(L) = 19.1$  cm in 20 s. Table 1 summarizes the initial state, steady-state, transition time and transition function of each boundary used in this experiment. We measured the transient head data at two intermediate points,  $x = 20$  cm and  $x = 30$  cm, using digital manometers with 0.01 cm H<sub>2</sub>O resolution.

To quantitatively assess our framework, we calculated  $\alpha$ ,  $\beta$ ,  $A$  and  $B$  to give,

$$\alpha = h_\infty(0) - h_0(0), \quad (33)$$

$$\beta = h_\infty(L) - h_0(L), \quad (34)$$

$$A = \frac{-1}{\alpha} \left[ \frac{1}{3} aM^3 + \frac{1}{2} bM^2 + (c - h_\infty(0))M \right], \quad (35)$$

$$B = \frac{N}{2}. \quad (36)$$

**Table 1**  
Experiment 1: Laboratory data for linearly varying right and quadratically varying left boundary conditions.

	Initial head (cm)	Steady state head (cm)	Transition time (s)	Transition function (cm)
Left boundary	22.5	19.1	3	$B_L(t) = 0.37t^2 - 2.22t + 22.48$
Right boundary	22.5	19.1	20	$B_R(t) = -0.17t + 22.50$

**Table 2**  
Experimental and theoretical values of MAT,  $\sqrt{VAT}$  and  $MAT + \sqrt{VAT}$  at  $x = 20$  cm and  $x = 30$  cm for Experiment 1.

	MAT		$\sqrt{VAT}$		$MAT + \sqrt{VAT}$	
	$x = 20$	$x = 30$	$x = 20$	$x = 30$	$x = 20$	$x = 30$
Experimental values (s)	12.3	14.3	9.1	8.7	21.4	23.0
Theoretical values (s)	11.2	14.3	10.4	8.6	21.6	22.9

Values of  $\alpha$ ,  $\beta$ ,  $A$  and  $B$  for this experiment were calculated as  $-3.4$  cm,  $-3.4$  cm,  $1.1$  s and  $10.0$  s, respectively. Using Eq. (17), we predict that the MAT at  $x = 20$  cm and  $x = 30$  cm are  $T(20) = 11.2$  s and  $T(30) = 14.3$  s, respectively. Similarly, after using Eqs. (23) and (24) and evaluating the constants  $C = 0.4$  and  $E = 33.3$ , Eq. (25) gives  $\sqrt{V(20)} = 10.4$  s and  $\sqrt{V(30)} = 8.6$  s, respectively.

Predictions of MAT and  $\sqrt{VAT}$  are summarized in Table 2. To test these predictions, we analyzed our laboratory data from Experiment 1 at  $x = 20$  cm and  $x = 30$  cm, as shown in Fig. 3. To compute  $f(t; x)$ , we used the data from Fig. 3(a) and (b). We apply Eq. (10), using a central difference approximation to estimate  $\partial h / \partial t$  (Chapra and Canale, 2009). Our estimates of  $t \times f(t; x)$  at  $x = 20$  cm and  $x = 30$  cm are given in Fig. 3(c) and (d). We applied Eqs. (11) and (18) to estimate  $T(x)$  and  $V(x)$  using the trapezoidal rule (Chapra and Canale, 2009) to estimate the integrals. The results are summarized in Table 2. Our results, reported in Fig. 3(a) and (b), shows that the predicated effective time scale,  $MAT + \sqrt{VAT}$ , is a good approximation for the time required for the system to effectively reach steady-state. Furthermore, the

**Table 3**  
Experiment 2: Laboratory data for linearly varying right and fixed left boundary conditions.

	Initial head (cm)	Steady state head (cm)	Transition time (s)	Transition function (cm)
Left boundary	25.0	25.0	-	$B_L(t) = 22.50$
Right boundary	25.0	23.0	25	$B_R(t) = -0.08t + 25.0$

**Table 4**  
Experimental and theoretical values of MAT,  $\sqrt{VAT}$  and  $MAT + \sqrt{VAT}$  at  $x = 20$  cm and  $x = 30$  cm for Experiment 2.

	MAT		$\sqrt{VAT}$		$MAT + \sqrt{VAT}$	
	$x = 20$	$x = 30$	$x = 20$	$x = 30$	$x = 20$	$x = 30$
Experimental values (s)	19.2	18.3	8.2	8.3	27.4	26.6
Theoretical values (s)	19.4	17.7	9.9	9.7	29.3	27.4

results in Table 2 show that the predicted estimates of MAT and VAT compare well with the values estimated directly from the experimental data set.

3.2. Experiment 2: Laboratory data for Case II

In this experiment, a fixed boundary condition was maintained in the left chamber, and a linearly varying boundary condition at the right chamber. We used Eq. (31) to model the right boundary condition. A pump was used to evacuate water from the right chamber at a uniform rate. As shown in Table 3, in this experiment, the following conditions were used:  $h_0(x) = 25$  cm,  $h_\infty(L) = 23$  cm and  $N = 25$  s for the right boundary condition.

To quantitatively assess our MAT predictions, we first calculated the constant  $B$  defined by Eq. (16) as  $B = N/2 = 12.5$  s. Using Eq. (29) we found  $T(20) = 19.4$  s and  $T(30) = 17.7$  s, respectively. Similarly, applying Eq. (24) we found  $E = N^2/12 = 52.1$  s<sup>2</sup> and  $\sqrt{V(20)} = 9.9$  s and  $\sqrt{V(30)} = 9.7$  s, respectively, using Eq. (30). Our predictions of MAT and  $\sqrt{VAT}$  values are summarized in Table 4. The transient data collected from Experiment 2 are

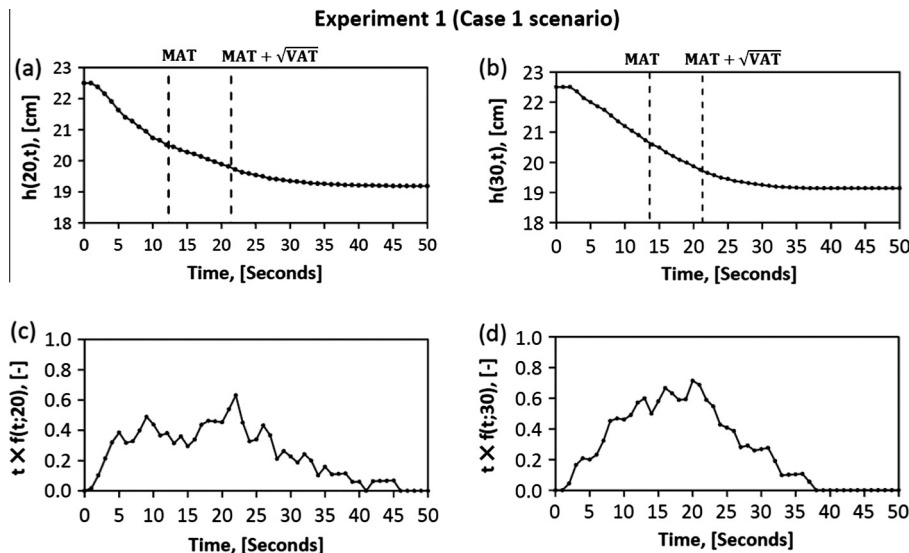


**Fig. 3.** Laboratory data for Experiment 1 with initial condition  $h_0(x) = 22.5$  cm, the left boundary condition varying quadratically from  $h_0(0) = 22.5$  to  $h_0(L) = 19.1$  in 3 s, and the right boundary condition varying linearly from  $h_0(L) = 22.5$  cm to  $h_\infty(L) = 19.1$  cm in 20 s. Results in (a) and (b) show the observed head changes at  $x = 20$  cm and  $x = 30$  cm, respectively. Results in (c) and (d) show  $t \times f(t; 20)$  and  $t \times f(t; 30)$ ; where  $f(t; x)$  is the probability density function at location  $x$ . Integrating  $t \times f(t; x)$  provides an estimate of the MAT at position  $x$ . An improved estimate of the effective time scale required for the system to reach steady-state is:  $MAT(x) + \sqrt{VAT(x)}$ .

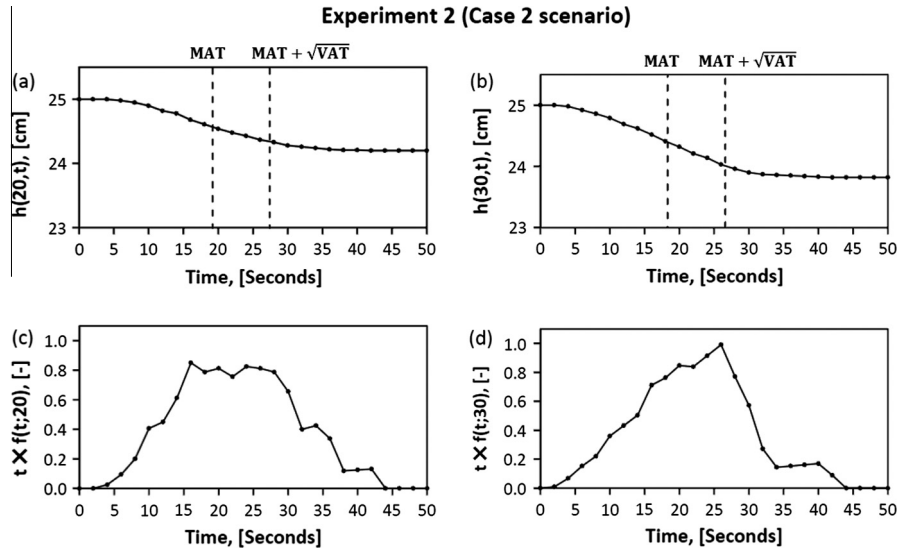


**Fig. 4.** Laboratory data for Experiment 2 with initial condition  $h_0(x) = 25$  cm, the left boundary condition fixed at  $B_L(t) = 25$  cm, and the right boundary condition varying linearly from  $h_0(L) = 22.5$  cm to  $h_\infty(L) = 23$  cm in 25 s. Results in (a) and (b) show the observed head changes at  $x = 20$  cm and  $x = 30$  cm, respectively. Results in (c) and (d) show  $t \times f(t; 20)$  and  $t \times f(t; 30)$ ; where  $f(t; x)$  is the probability density function at location  $x$ . Integrating  $t \times f(t; x)$  provides an estimate of the MAT at position  $x$ . An improved estimate of the effective time scale required for the system to reach steady state is:  $MAT(x) + \sqrt{VAT(x)}$ .

reported in Fig. 4. Similar to Experiment 1, MAT,  $\sqrt{VAT}$  and  $MAT + \sqrt{VAT}$  at  $x = 20$  cm and  $x = 30$  cm were calculated and the results were compared against theoretical predictions. As shown in Table 4, the theoretical predictions are in good agreement with experimental results. Results in Fig. 4(a) and (b) illustrate that the predicted time scale required for the system to effectively reach steady-state,  $MAT + \sqrt{VAT}$ , is consistent with our experimental observations.

#### 4. Summary and conclusions

The focus of this study is to present a mathematical framework which can predict the response time scales of groundwater flow near a groundwater surface-water interface. To achieve this we applied the theory of MAT (McNabb and Wake, 1991) to estimate the time scale required for flow in a one-dimensional aquifer to respond to various types of surface-water boundary perturbations. We tested the proposed framework using two data sets collected from a laboratory-scale experiment. Results show that the experimental data are in good agreement with model predictions. A key limitation of previous approaches for estimating the response time scales is that they gave no simple framework for studying the sensitivity of the time scale to various system parameters. Alternatively, our MAT framework provides a relatively straightforward mathematical relationship between the response time scale and various system parameters.

The limitations of our framework are that the boundary conditions must vary monotonically and that they must approach some steady value faster than  $t^{-1}$  decays to zero as  $t \rightarrow \infty$ . Furthermore, we also require that both boundary conditions must either increase or decrease, or that one of the boundary conditions remains fixed. In practice, these limitations are not overly restrictive and a wide range of transient groundwater problems can be analyzed using the proposed framework. We also acknowledge that for all systems considered in this work we always considered an initial condition,  $h_0(x)$ , that was spatially constant, independent of position. We note that the same mathematical procedure used to find MAT and VAT also applies to other conditions where the initial condition is genuinely spatially variable and these mathematical details can be found in our previous work (Ellery et al., 2012).

#### Acknowledgements

This work was, in part, supported by a National Science Foundation Grant, NSF-EAR-0943679B. FJ was also supported by the Auburn University graduate student assistantship program. MJS was supported by the Australian Research Council (FT130100148). We appreciate the support from the School of Mathematical Sciences at QUT. FJ and TPC acknowledge Nicholas Lowe for his valuable help in conducting the laboratory experiments and gathering data. FJ conducted the laboratory experiments, derived the governing equations, developed the first draft of the manuscript, and worked on subsequent revisions. MJS provided ideas, assisted with mathematical derivations and revised multiple drafts of this manuscript. TPC helped with experiments, suggested ideas, and revised multiple drafts of the manuscript. Based on Clement's (2014) approach, the relative contributions are estimated to be FJ (50%), MJS (25%) and TPC (25%).

#### Appendix A. Notation (SI units)

The following notation is used in this paper:

- $a, b, c$ , quadratic coefficients; ( $m/s^2$ ), ( $m/s$ ), ( $m$ )
- $A = \frac{1}{\alpha} \int_0^\infty (h_\infty(0) - B_L(t)) dt$ ; (s)
- $B = \frac{1}{\beta} \int_0^\infty (h_\infty(L) - B_R(t)) dt$ ; (s)
- $C = \frac{1}{\alpha} \int_0^\infty \frac{dB_L(t)}{dt} (t - A)^2 dt$ ; ( $s^2$ )
- $D$ , aquifer diffusivity; ( $m^2/s$ )
- $E = \frac{1}{\beta} \int_0^\infty \frac{dB_R(t)}{dt} (t - B)^2 dt$ ; ( $s^2$ )
- $F(t; x)$ , cumulative distribution function; (-)
- $f(t; x)$ , probability distribution function; ( $1/s$ )
- $g(x) = h_\infty(x) - h_0(x)$ ; ( $m$ )
- $h(x, t)$ , groundwater head at point  $x$  and time  $t$ ; ( $m$ )
- $h_0(x)$ , initial groundwater head; ( $m$ )
- $h_0$ , horizontal initial condition in laboratory experiments; ( $m$ )
- $h_\infty(x)$ , steady state groundwater head; ( $m$ )
- $h_0(0), h_0(L)$ , initial groundwater head at the left and right boundary conditions; ( $m$ )
- $h_\infty(0), h_\infty(L)$ , steady state groundwater head at the left and

(continued on next page)

right boundary conditions; (m)  
 $\bar{h}$ , average saturated thickness; (m)  
 $K$ , saturated hydraulic conductivity; (m/s)  
 $L$ , length of the aquifer; (m)  
 $M$ , right boundary condition transition time; (s)  
 $N$ , left boundary condition transition time; (s)  
 $B_L(t)$ ,  $B_R(t)$ , left and right varying boundary conditions; (m)  
 $S_y$ , aquifer specific yield; (–)  
 $T(x)$ , mean action time (MAT); (s)  
 $V(x)$ , variance of action time (VAT); ( $s^2$ )  
 $w_a$ ,  $w_b$ , weight functions of  $A$  and  $B$ , respectively; (m)  
 $\alpha = h_\infty(0) - h_0(0)$ ; (m)  
 $\beta = h_\infty(L) - h_0(L)$ ; (m)  
 $\gamma$ ,  $\delta$ ,  $\eta$ ,  $\theta$ , parameters used to calculate  $V(x)$ ; ( $m^4 s$ ), ( $m^4 s$ ), ( $m^4 s$ ), ( $s^2$ )  
 $\psi(x) = g(x)[V(x) + T(x)^2]$ ; ( $m s^2$ )

## References

- Abarca, E., Clement, T.P., 2009. A novel approach for characterizing the mixing zone of a saltwater wedge. *Geophys. Res. Lett.* 36, L06402.
- Bansal, R.K., 2005. *A Textbook of Fluid Mechanics and Hydraulic Mechanics*, ninth ed. Laxmi Publications, New Delhi.
- Barlow, P.M., Moech, A.F., 1998. Analytical solutions and computer programs for hydraulic interaction of stream-aquifer systems. US Geological Survey Open-File Report. 98-415A.
- Bear, J., 1979. *Hydraulics of Groundwater*. McGraw Hill, New York.
- Chang, S.W., Clement, T.P., 2012a. Experimental and numerical investigation of saltwater intrusion dynamics in flux-controlled groundwater systems. *Water Resour. Res.* 48 (9), W09527. <http://dx.doi.org/10.1029/2012WR012134>.
- Chang, S.W., Clement, T.P., 2012b. Laboratory and numerical investigation of transport processes occurring above and within a saltwater wedge. *J. Contam. Hydrol.* 147, 14–24.
- Chang, S.W., Clement, T.P., Simpson, M.J., Lee, K.K., 2011. Does sea-level rise have an impact on saltwater intrusion? *Adv. Water Resour.* 34, 1283–1291.
- Chapra, S.C., Canale, R.P., 2009. *Numerical Methods for Engineers*, sixth ed. McGraw Hill, Singapore.
- Clement, T.P., 2014. Authorship matrix – a rational approach to quantify individual contributions and responsibilities in multi-author scientific articles. *Sci. Eng. Ethics J.* 20, 345–361.
- Clement, T.P., Wise, W.R., Molz, F.J., 1994. A physically based, two-dimensional, finite-difference algorithm for variably-saturated flow. *J. Hydrol.* 161, 71–90.
- Ellery, A.J., Simpson, M.J., McCue, S.W., Baker, R.E., 2012a. Critical time scales for advection–diffusion–reaction processes. *Phys. Rev. E* 85, 041135.
- Ellery, A.J., Simpson, M.J., McCue, S.W., Baker, R.E., 2012b. Moments of action provide insight into critical times for advection–diffusion–reaction processes. *Phys. Rev. E* 86, 031136.
- Ellery, A.J., Simpson, M.J., McCue, S.W., Baker, R.E., 2013. Simplified approach for calculating moments of action for linear reaction–diffusion equations. *Phys. Rev. E* 88, 054102.
- Haberman, R., 2004. *Applied Partial Differential Equations: With Fourier Series and Boundary Value Problems*. Prentice Hall.
- Hantush, M.M., 2005. Modeling stream-aquifer interactions with linear response functions. *J. Hydrol.* 311 (1–4), 59–79.
- Hickson, R.L., Barry, S.I., Mercer, G.N., 2009a. Critical times in multilayer diffusion. Part 1: Exact solutions. *Int. J. Heat Mass Transf.* 52, 5776–5783.
- Hickson, R.L., Barry, S.I., Mercer, G.N., 2009b. Critical times in multilayer diffusion. Part 2: Approximate solutions. *Int. J. Heat Mass Transf.* 52, 5784–5791.
- Hickson, R.L., Barry, S.I., Sidhu, H.S., Mercer, G.N., 2011. Critical times in singlelayer reaction diffusion. *Int. J. Heat Mass Transf.* 54, 2642–2650.
- Landman, K.A., McGuinness, M.J., 2000. Mean action time for diffusive processes. *J. Appl. Math. Decis. Sci.* 4, 125–141.
- Lockington, D.A., 1997. Response of unconfined aquifer to sudden change in boundary head. *J. Irrig. Drain. Eng.* 123 (1), 24–27.
- Lu, C., Werner, A.D., 2013. Timescales of seawater intrusion and retreat. *Adv. Water Resour.* 59, 39–51.
- McNabb, A., 1993. Mean action times, time lags, and mean first passage times for some diffusion problems. *Math. Comput. Modell.* 18, 123–129.
- McNabb, A., Wake, G.C., 1991. Heat conduction and finite measure for transition times between steady states. *IMA J. Appl. Math.* 47, 193–206.
- Mishra, G.C., Jain, S.K., 1999. Estimation of hydraulic diffusivity in stream-aquifer system. *J. Irrig. Drain. Eng.* 125 (2), 74–81.
- Ojha, C.S.P., 2000. Explicit aquifer diffusivity estimation using linearly varying stream stage. *J. Hydrol. Eng.* 5 (2), 218–221.
- Pinder, G.F., Bredehoeft, J.D., Cooper, H.H., 1969. Determination of aquifer diffusivity from aquifer response to fluctuations in river stage. *Water Resour. Res.* 5 (4), 850–855.
- Rodriguez, L.B., Cello, P.A., Vionnet, C.A., 2006. Modeling stream-aquifer interactions in shallow aquifer, Choele Choele Island, Patagonia, Argentina. *Hydrogeol. J.* 14, 591–602.
- Rowe, P.P., 1960. An equation for estimating transmissibility and coefficient of storage from river-level fluctuations. *J. Geophys. Res.* 65 (10), 3419–3424.
- Simpson, M.J., Clement, T.P., Gallop, T.A., 2003a. Laboratory and numerical investigation of flow and transport near a seepage-face boundary. *Ground Water* 41 (5), 690–700.
- Simpson, M.J., Clement, T.P., Feomans, F.E., 2003b. Analytical model for computing residence times near a pumping well. *Ground Water* 41 (3), 351–354.
- Simpson, M.J., Jazaei, F., Clement, T.P., 2013. How long does it take for aquifer recharge or aquifer discharge processes to reach steady state? *J. Hydrol.* 501, 241–248.
- Singh, S.R., Sagar, B., 1977. Estimation of aquifer diffusivity in stream-aquifer systems. *J. Hydraul. Div. ASCE* 103 (11), 1293–1302.
- Sophocleous, M., 2012. On understanding and predicting groundwater response time. *Ground Water* 50 (4), 528–540.
- Srivastava, R., 2003. Aquifer response to linearly varying stream stage. *J. Hydrol. Eng.* 8 (6), 361–364.
- Swamee, P., Singh, S., 2003. Estimation of aquifer diffusivity from stream stage variation. *J. Hydrol. Eng.* 8 (1), 20–24.
- Watson, T.A., Werner, A.D., Simmons, C.T., 2010. Transience of seawater intrusion in response to sea level rise. *Water Resour. Res.* 46, W12533.
- Winter, T.C., 1995. Recent advances in understanding the interaction of groundwater and surface water. *Rev. Geophys.* 33 (S2), 985–994.